

Fuzzy-PI Torque and Flux Controllers for DTC with Multilevel Inverter of Induction Machines

N. M. Nordin¹, N. R. N. Idris², N. A. Azli³, M. Z. Puteh⁴, T. Sutikno⁵

^{1,2,3}Faculty of Electrical Engineering, Universiti Teknologi Malaysia, Johor Bahru, Malaysia

⁴MIMOS Berhad, Technology Park Malaysia, Kuala Lumpur, Malaysia

⁵Department of Electrical Engineering, Universitas Ahmad Dahlan, Yogyakarta, Indonesia

Article Info

Article history:

Received Aug 19, 2014

Revised Sep 20, 2014

Accepted Oct 1, 2014

Keyword:

CMLI

Direct torque control

Fuzzy logic control

Induction machines

Multilevel inverter

ABSTRACT

In this paper the performance of flux and torque controller for a Direct Torque Control of Cascaded H-bridge Multilevel Inverter (DTC-CMLI) fed induction machines are investigated. A Fuzzy-PI with fixed switching frequency is proposed for both torque and flux controller to enhance the DTC-CMLI performance. The operational concepts of the Fuzzy-PI with the fixed switching frequency controller of a DTC-MLI system followed by the simulation results and analysis are presented. The performance of the proposed system is verified via MATLAB/Simulink[®]. The proposed system significantly improves the DTC drive in terms of dynamic performance, smaller torque and flux ripple, and lower total harmonic distortion (THD).

*Copyright © 2014 Institute of Advanced Engineering and Science.
All rights reserved.*

Corresponding Author:

Nik Rumzi Nik Idris,

Departement of Electrical Power Engineering,

Faculty of Electrical Engineering, Universiti Teknologi Malaysia,

81310 Skudai, Johor, Malaysia.

Email: nikrumzi@ieee.org / nikrumzi@fke.utm.my

1. INTRODUCTION

The superior performance of DTC in dynamic response and simple control configuration which is originally introduced in [1], has made it one of the most popular research topics in electrical drive systems. Since the application of high-power medium voltage in AC drives has shown rapid development, the use of multilevel inverters in DTC scheme has become an important structure for further development and improvement. Various technical papers have shown better performance of DTC scheme using multilevel inverters [2-31].

By employing the multilevel inverter, the choices of voltage vectors that can be used to control the torque and flux are increased. Different approaches have been proposed for DTC scheme using multilevel inverter; hysteresis-based controller and non-hysteresis-based controller such as space vector modulation (SVM)[8, 13, 16, 18, 22, 27-29, 31], predictive control strategy [10, 12, 30] and fuzzy logic controller (FLC)[7, 9, 11, 22].

The implementation of the hysteresis-based control strategy has lead to a high torque ripple especially in discrete implementation even with small hysteresis band. This is due to the delay in the sampling time. On top of that, the variable switching frequency of the switching devices which leads to unpredictable harmonics current is also produced by implementing the hysteresis-based control strategy.

As a result, some researchers have chosen to use non-hysteresis-based control strategies to overcome these drawbacks. Significant improvements in terms of flux and torque ripple and switching frequency are accomplished by using these control strategies; however the use of complex mathematical equations and

algorithms has led to the computational burden and complexity of the DTC-MLI scheme especially when the level of voltage is increased.

In [6] the multilevel inverter in the DTC scheme employs a multilevel hysteresis controller. Although the results have shown some significant improvements, as mentioned earlier, by using the hysteresis-based controller the switching frequency of the power devices varies while the torque and flux ripple can still be considered as high. A fuzzy-PI based controller for DTC was initially introduced in [32]. The controller has been used to replace the hysteresis controller while maintaining the use of a look-up table. However the proposed controller has been applied to a 3-phase conventional inverter.

In this work a fuzzy-PI with the fixed switching frequency controller is utilized in the look-up table based DTC drive. The proposed controller consists of a fuzzy logic controller and a triangular carrier waveform. The fixed switching frequency is obtained by comparing the fuzzy logic output with the triangular waveforms. A 5-level cascaded H-bridge multilevel inverter (CMLI) is employed in this scheme. The multiple isolated input DC sources of the CMLI are particularly suitable for electric vehicle (EV) applications since the power source for an EV can be obtained from the battery modules. In the proposed strategy, the fuzzy-PI with the fixed switching frequency controller will replace the multilevel hysteresis controller for torque and flux control. Based on the proposed controller output together with the flux position, an appropriate voltage vector can be selected from the look-up table. Figure 1 shows a proposed system block diagram.

In this paper, the operational concepts of fuzzy-PI with the fixed switching frequency controller followed by the simulation results and analysis on the performance of the proposed system are presented. The results have shown that better dynamic performance, smaller torque and flux ripples, constant device switching frequency and lower THD in the phase current are achieved.

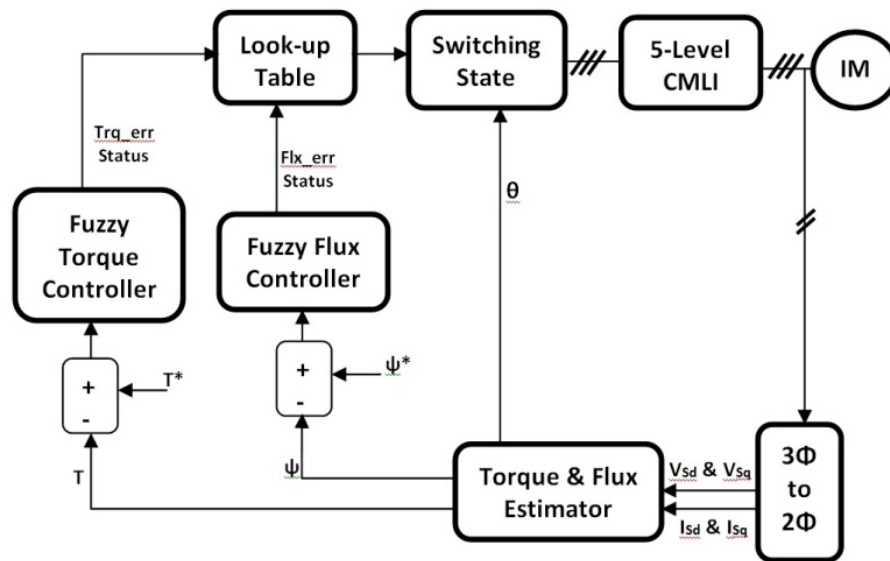


Figure 1. Proposed system block diagram

2. BASIC PRINCIPLE OF DIRECT TORQUE CONTROL (DTC)

In Figure 2 the block diagram of DTC basic control which originally introduced by [1] is shown. By having an instantaneous value of torque and flux which are calculated from the measured terminal variables of induction machine (IM), both torque and flux errors can be determined. Based on the errors, an optimum required voltage vectors are selected from the look-up tables to drive the IM.

The flux estimation is based on stator voltage vector equation in stationary reference frame which can be written as

$$\overline{v_s} = R_s \overline{i_s} + \frac{d\overline{\psi_s}}{dt} \quad (1)$$

Over the small period of time, it is assumed that the voltage drop across the stator resistance can be neglected. Therefore the equation can be rewritten as

$$\overline{v}_s = \frac{\Delta \overline{\psi}_s}{\Delta t} \tag{2}$$

It's clearly shows that the change in stator flux linkage vector, $\Delta \overline{\psi}_s$ is directly affected by the selection of stator voltage vector. Hence the stator flux locus can be controlled by selecting a suitable voltage vectors.

As for the torque estimation, it based on the stator-rotor flux angle movement. The relationship between stator-rotor flux angle and electromagnetic torque in stationary reference frame can be written as

$$T_e = \frac{3}{2} P \overline{\psi}_s \times \overline{i}_s = \frac{3}{2} P |\psi_s| |\psi_r| \sin \theta_{sr} \tag{3}$$

Where $|\psi_s|$ and $|\psi_r|$ are the magnitudes of stator flux and rotor flux linkages respectively and θ_{sr} is the stator-rotor flux angle. When a voltage vector is applied, the stator flux linkage will move faster than rotor flux linkage, where the rotor flux motion is lag behind the stator flux rotation. This is due to the to the rotor and stator leakage inductances. Therefore the stator-rotor flux angle, θ_{sr} (hence torque) is affected by the selection of appropriate voltage vector.

The abovementioned principle of both stator flux and stator-rotor angle movement are affected by the variation of stator voltage is used in DTC scheme to achieve a desired flux trajectory and torque response.

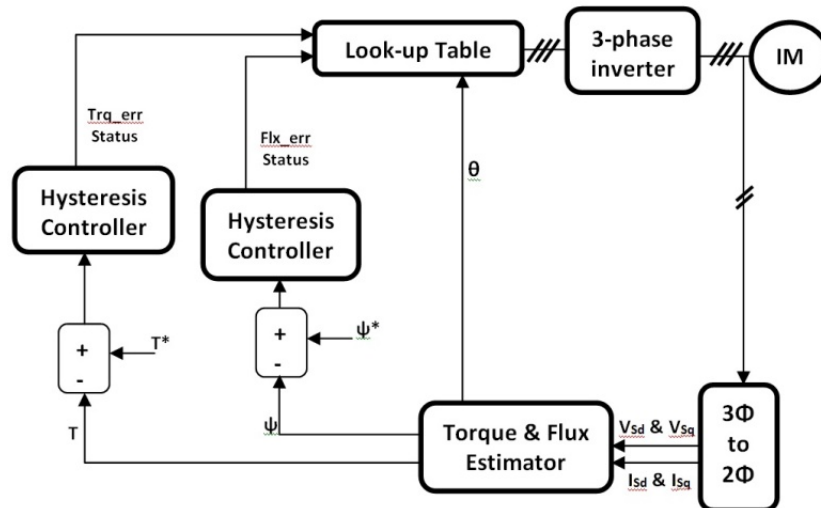


Figure 2. Conventional DTC block diagram

3. 5 LEVEL CASCADED H-BRIDGE MULTILEVEL INVERTER

5-level CMLI consist of 2 H-bridge inverter (cell) connected in cascaded form with separated DC source as shown in Figure 3. As for three-phase IM, each phase is fed by one 5-level CMLI. The configuration of three-phase IM fed by 5-level CMLI is shown in Figure 4.

The number of voltage level, L for CMLI can be obtained by

$$L = 2n + 1 \tag{4}$$

Where n is a number of cell per phase. Each cell is connected in series. Therefore the total output voltage of each phase can be determined by

$$V_{aN} = \sum_{n=1}^2 V_{an} \tag{5}$$

$$V_{bN} = \sum_{n=1}^2 V_{bn} \tag{6}$$

$$V_{cN} = \sum_{n=1}^2 V_{cn} \tag{7}$$

V_{aN} , V_{bN} and V_{cN} is the phase output voltage with respect to the neutral, N . By considering each cell produce $\{-V_{DC}, 0, V_{DC}\}$, based on (5), (6) and (7), a 5-level output voltage for each phase is

$$V_{aN} = V_{bN} = V_{cN} = \{-2V_{DC}, -V_{DC}, 0, V_{DC}, 2V_{DC}\} \tag{8}$$

The output voltages, V_s generated by the inverter can be expressed in space phasor form as given in (9).

$$V_s(t) = 2/3 (V_{aN}(t) + aV_{bN}(t) + a^2 V_{cN}(t)) \tag{9}$$

Where $a = e^{j2\pi/3}$ and $a^2 = e^{j4\pi/3}$. In d-q form, the output voltages can be defined as

$$V_{sd} = \frac{1}{3}(2V_{aN} - V_{bN} - V_{cN}) \tag{10}$$

$$V_{sq} = \frac{1}{\sqrt{3}}(V_{bN} - V_{cN}) \tag{11}$$

Based on 5-level multilevel inverter, $5^3 = 125$ combinations of phase voltage with $3L(L - 1) + 1 = 61$ voltage vectors can be generated. This can give more degrees of freedom in choosing voltage vectors for control purposes compared to the conventional 3-phase inverter. The higher the level of multilevel inverter, the more the voltage vectors generated. Figure 5 illustrates the voltage vectors generated by 5-level CMLI on a d-q plane.

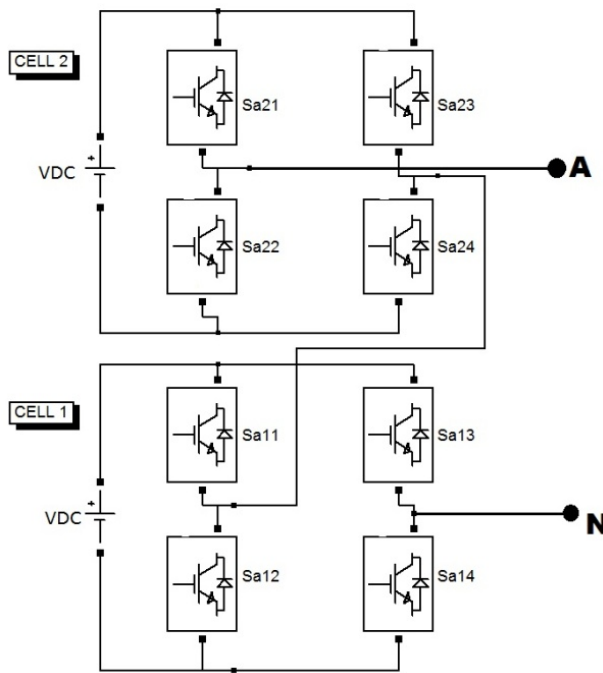


Figure 3. 5-level cascaded H-bridge multilevel inverter (CMLI)

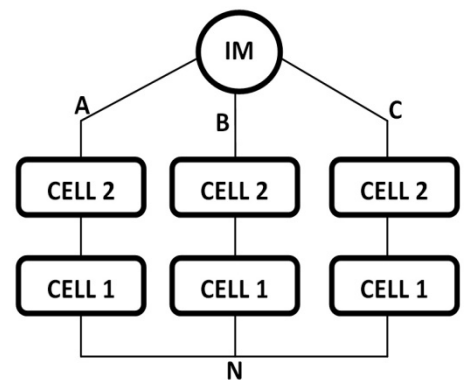


Figure 4. Three-phase IM fed by 5-level CMLI

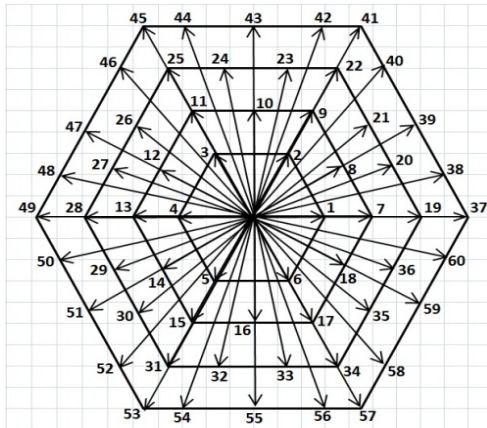


Figure 5. Voltage vector generated by 5-level CMLI

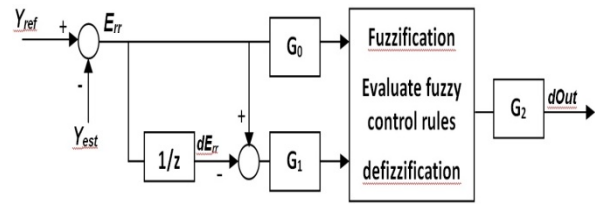


Figure 6. General structure of the Fuzzy-PI controller

4. THE PROPOSED CONTROLLER

The proposed controller is employed as an alternative to the hysteresis-based controller with the benefit of operating at a fixed switching frequency with low torque and flux ripple. Prior knowledge of rotor parameters is not required in designing a fuzzy-PI based controller. However, the fuzzy-PI performance is highly affected by the normalization gain selection of a typical fuzzy logic controller.

The fuzzy-PI controller structure is based on the traditional PI controller [33]. The general structure of the Fuzzy-PI controller is as shown in Figure 6. It has two inputs; system error, E_{rr} and the change of system error, dE_{rr} , where $E_{rr} = Y_{ref} - Y_{est}$ and $dE_{rr} = E_{rr}(t) - E_{rr}(t-\Delta t)$. Before these input values are fed into the fuzzy controller, both values need to be normalized by using the *input normalization gain* (G_0 and G_1). As for the fuzzy controller output, $dOut$, the value need to be denormalized using the *output denormalization gain*, G_2 before it can be used as a comparator input.

4.1 Fuzzy-PI torque controller

The proposed fuzzy-PI torque controller (FTC) consists of 6 triangular waveform generators, 6 comparators and a fuzzy-PI controller. The six triangular waveform generators generate 3 pairs of triangular waveforms with the same magnitude but with different DC offset. Each pair (C_{Upper} and C_{Lower}) is 180° out of phase. In principle, the proposed controller will produce the same output as an 8-level hysteresis controller in [6], which can be either one of the following torque error status; 3, 2, 1, +0.5, -0.5, -1, -2, -3. The number of levels, however, must be realistic enough for implementation purposes. In other words, the higher the number of levels, the faster in terms of processor requirement is needed for implementation. By comparing the triangular waveforms with the fuzzy-PI controller output, a fixed switching frequency can be achieved.

Based on the general structure of fuzzy-PI controller, the FTC has two inputs; torque error, T_{err} and the change of torque error, dT_{err} , where $T_{err} = T_{ref} - T_{est}$ and $dT_{err} = T_{err}(t) - T_{err}(t-\Delta t)$ and one output, dT_O . Figure 7 shows the block diagram of the FTC.

4.2 Fuzzy-PI flux controller

The proposed fuzzy-PI flux controller (FFC) consists of 4 triangular waveform generators, 4 comparators and a fuzzy-PI controller. The four triangular waveform generators generate 2 pairs of triangular waveforms with the same magnitude but with different DC offset and similar to the FTC, each pair (C_{Upper} and C_{Lower}) is also 180° out of phase. In principle, the proposed controller will produce the same output as a 5-level hysteresis controller in [6], which can be either one of the following torque error status; 2, 1, 0, -1, -2. Again, the number of levels chosen must be practical for implementation purposes.

Based on the general structure of fuzzy-PI controller, the FFC has two inputs; flux error, Flx_{err} and the change of flux error, $dFlx_{err}$, where $Flx_{err} = Flx_{ref} - Flx_{est}$ and $dFlx_{err} = Flx_{err}(t) - Flx_{err}(t-\Delta t)$ and one output, $dFlx_O$. Figure 8 shows a block diagram of FFC.

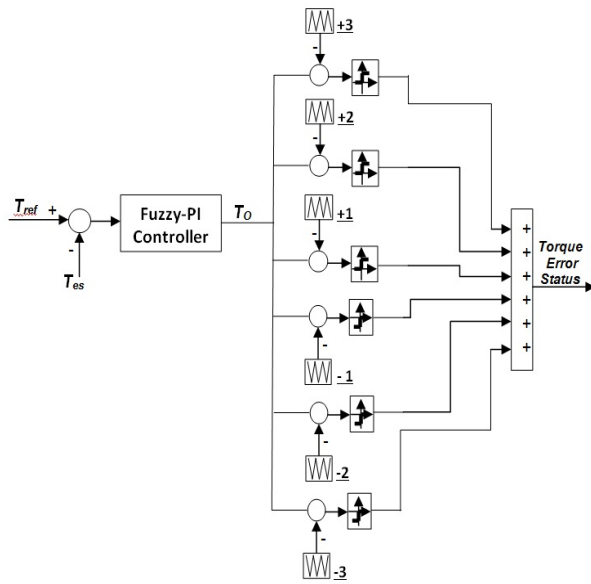


Figure 7. Fuzzy torque controller (FTC) block diagram

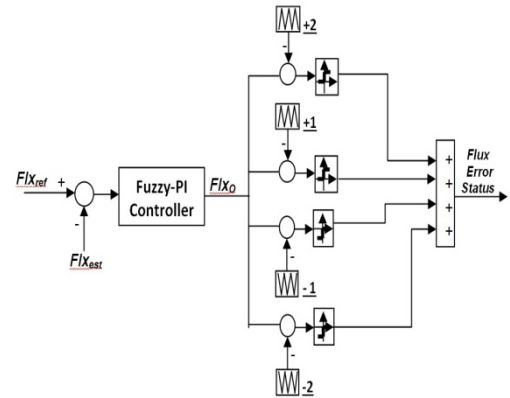


Figure 8. Fuzzy flux controller (FFC) block diagram

4.3 Fuzzification of inputs and outputs

Both FTC and FFC are using the same fuzzy control properties. The universe of discourse (UOD) for the inputs and outputs are divided into 7 overlapping subsets, +3 to -3. Table 1 shows the definitions of the fuzzy subsets in UOD.

Figure 9 shows the inputs and output membership functions of the fuzzy controller. Both inputs and outputs are connected through the rules that emulate an ideal second order system response which is expected to have good performance (response time, overshoot, damping factor and etc.) and system stability. By using the IF-THEN rules, the inputs and outputs are connected using 49 rules since 7 overlapping subsets are used. These rules are summarized and presented in the decision table as shown in Table 2.

Table 1. Fuzzy subsets definitions

Symbol	Linguistic Terms	Fuzzy Subsets
PL	Positive Large	+3
PM	Positive Medium	+2
PS	Positive Small	+1
Z	Zero	0
NS	Negative Small	-1
NM	Negative Medium	-2
NL	Negative Large	-3

Table 2. Decision table of fuzzy control rules

T_err/Flx_err \ dT_err/dFlx_err	T_err/Flx_err						
	PL	PM	PS	Z	NS	NM	NL
PL	PL	PL	PM	PM	PS	PS	Z
PM	PL	PM	PM	PS	PS	Z	NS
PS	PM	PM	PS	PS	Z	NS	NS
Z	PM	PS	PS	Z	NS	NS	NM
NS	PS	PS	Z	NS	NS	NM	NM
NM	PS	Z	NS	NS	NM	NM	NL
NL	Z	NS	NS	NM	NM	NL	NL

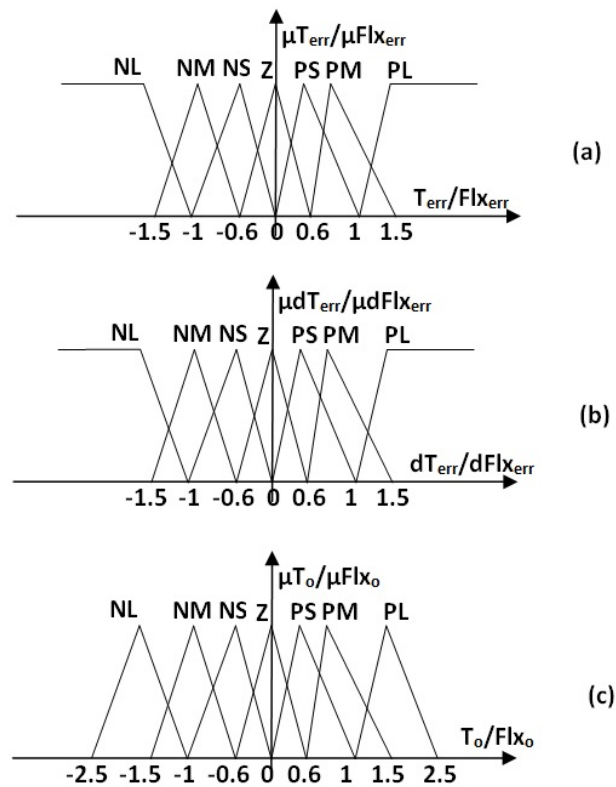


Figure 9. Membership functions of the fuzzy controller
 (a) First input variable (b) Second input variable (c) Output variables

4.4 Fuzzy controller gain selection

In order to get a smaller torque and flux ripple and fixed switching frequency, the fuzzy controller gain must be properly selected to fulfill two main criteria of torque and flux controller:

- Produce a good dynamics of flux and torque response.
- Absolute slope of the torque and flux controller output (T_o and Flx_o) must not exceed the absolute slope of the triangular carrier to avoid multiple intersection and hence extremely high switching frequency.

By using trial and error method, several combinations of gain (G_0 , G_1 , G_2) have been found to achieve the desired response. In general, lower values of G_0 and G_1 must be accompanied with a higher value of G_2 and vice versa.

The characteristic of each gain towards the system's response can be clearly understood by referring to Table 3. In this table, the changes of G_0 and G_1 will affect the torque and flux response time and the controller output slope. Therefore the G_2 value needs an opposite adjustment to compensate the incremental or decremental effect produced by G_0 and G_1 in order to achieve the desired response. Fig. 10 shows an example of fuzzy controller output (T_o or Flx_o) with proper gain value.

Table 3. General response of fuzzy controller gain with the increasing and decreasing values of G_0 , G_1 and G_2 .

↑↑ and ↓↓ Denotes highly effected ↑ and ↓ Denotes moderately effected

Gain	Torque & Flux Response		Slope of T_o and Flx_o
	Response time	Ripple	
G_0	Increasing	↑↑	↑↑
	Decreasing	↓↓	↓↓
G_1	Increasing	↓	↑↑
	Decreasing	↑	↓↓
G_2	Increasing	↑↑	↑↑
	Decreasing	↓↓	↓↓

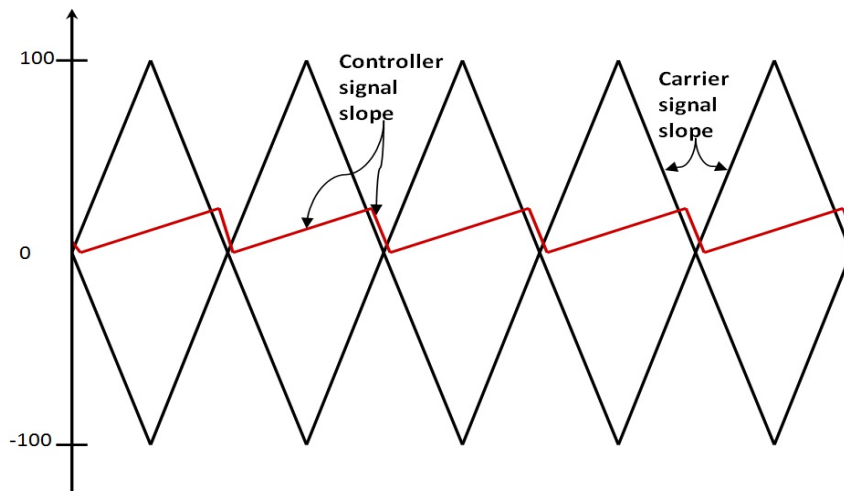


Figure 10. Fuzzy controller output with proper gain

5. SIMULATION RESULTS

The proposed system and a hysteresis-based system have been simulated using MATLAB/Simulink for validation purposes. Both systems use the same induction machines parameters as shown in Table 4.

For the hysteresis-based system, the flux and torque hysteresis band is set to 10% of the rated values. As for the Fuzzy-PI-based controller, the values of G_0 , G_1 and G_2 are set to 0.15, 0.01, 400 and 4, 0.008, 3000, for fuzzy torque and fuzzy flux controller respectively. The triangular carrier waveforms frequencies for flux and torque fuzzy-PI based controller are 5 kHz and 10 kHz respectively.

5.1 Torque and flux step response

A step reference torque and flux at $t = 0.01s$ has been applied to the DTC-CMLI system. Figure 11 and Figure 12 show a step response of flux and torque for both controllers respectively. It's clearly indicated that the proposed controller responds faster than the hysteresis controller where both torque and flux with proposed controller achieved steady state at 0.0171s and 0.145s respectively while both torque and flux with hysteresis controller achieved steady state at 0.0176s and 0.0151s respectively.

In the proposed controller (DTC-CMLI with fuzzy-PI controller), the designated fuzzy rules first filtered and processed the error (torque and flux) to ensure the large error will appropriately trigger the correct triangular. Consequently, the voltage vector with highest torque and flux increment (decrement) is selected for large errors hence produce faster torque and flux response.

As for DTC-CMLI with hysteresis controller, the errors are directly controlled by hysteresis controller which produces a slower response compared to proposed controller.

Table 4. Parameter used in simulation

Induction Motor parameters		Cascaded H-Bridge Multilevel Inverter parameters	
Nominal Power	1.5 kW	V_{DC} for each cell	120 V
$V_{line-line}$ (rms)	400Vrms 50 Hz	Power electronic device	IGBT
Stator Resistance	3 Ω	Reference value	
Rotor Resistance	3.793 Ω	Torque reference	9 N.m
Stator Inductance	0.322188 H	Flux reference	0.9 Wb
Rotor Inductance	0.330832 H		
Mutual Inductance	0.3049 H		
Inertia	0.02799 kg.m ²		
Friction Factors	0.01025 N.m.s		
Pole	2 pole		

5.2 Torque and flux ripple

Figure 13 and Figure 14 show the flux and torque peak-to-peak ripples respectively for both proposed controller and hysteresis controller. These figures clearly indicate the reduction of torque and flux ripple as much as 10% in the proposed controller compared to the hysteresis controller.

Using the proposed controller in the system, the designated fuzzy rules for torque and flux controller are properly monitored and corrected the level of errors to ensure that the output fuzzy controller signals are within the appropriate triangle level hence appropriate voltage vector either to increase or decrease torque or flux is selected and been applied consecutively within a triangle waveform period.

However by using the hysteresis controller in the system, the voltage vector is chosen based on the comparison of raw error signal with the hysteresis band which the voltage vector for torque and flux increasing or decreasing are applied for entire switching period.

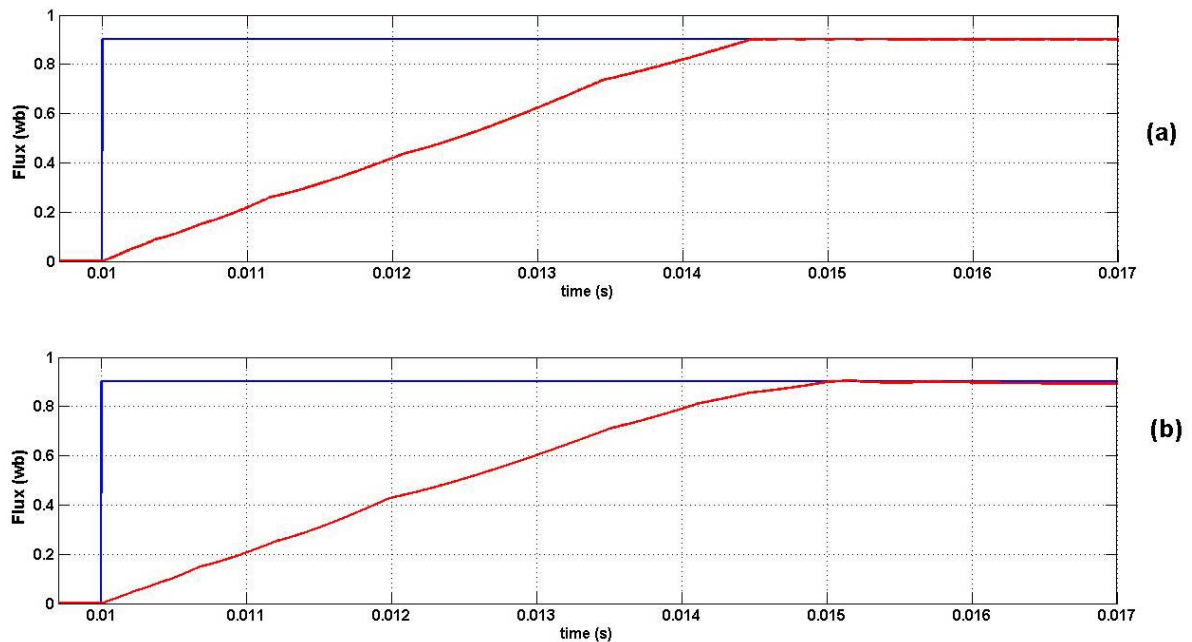


Figure 11. Stator flux step response (a) Proposed controller (b) Hysteresis controller

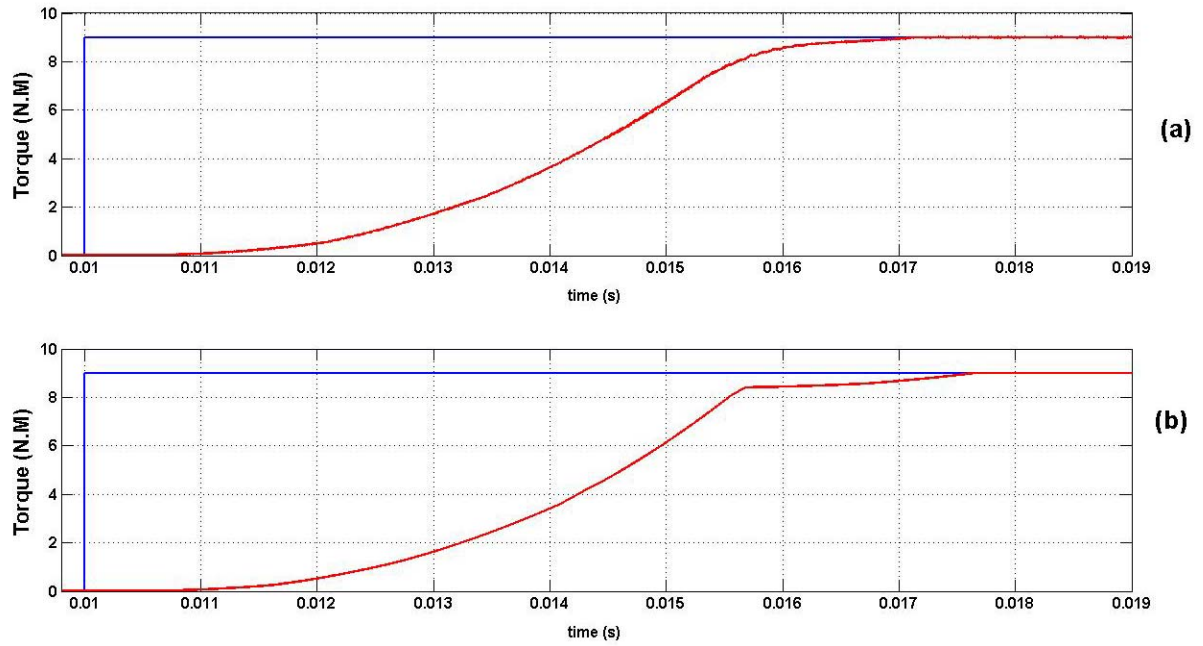


Figure 12. Torque step response (a) Proposed controller (b) Hysteresis controller

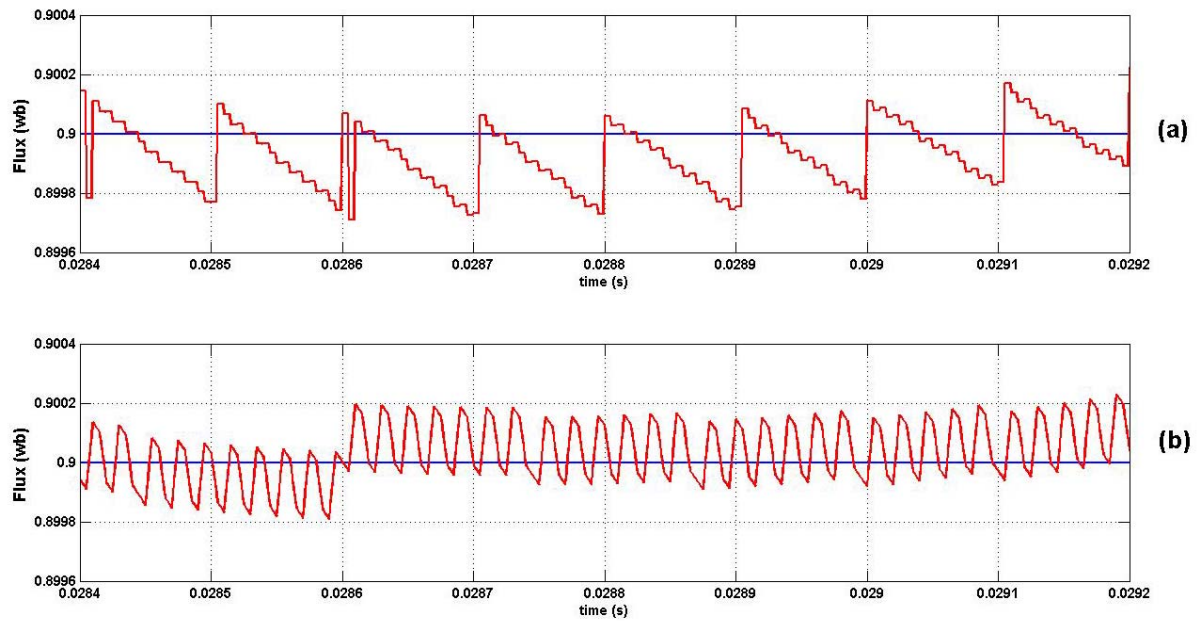


Figure 13. Stator flux ripple (a) Proposed Controller (b) Hysteresis Controller

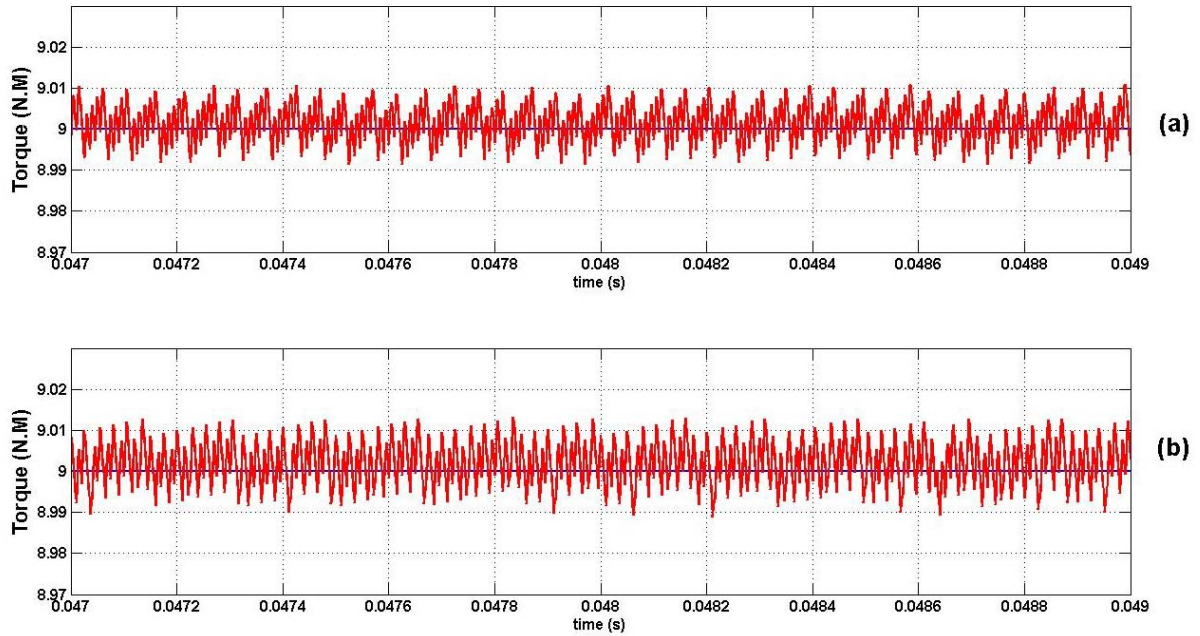


Figure 14. Torque ripple (a) Proposed Controller (b) Hysteresis Controller

5.3 Switching frequency and THD in stator phase current

Figure 15 (a) and (b) show the frequency spectrum of the switching pattern, S_{b23} for both proposed controller and hysteresis controller respectively. DTC-CMLI with hysteresis controller suffers from the varying device switching frequency. Variable switching frequency is undesirable since the switching capability of the inverter is not fully utilized. Furthermore create an unpredictable harmonics in current flow. Based on the spectrum in Figure 15 (b), the harmonics are widely distributed.

On the contrary, DTC-CMLI with proposed controller offers a constant switching frequency. Based on the spectrum in Fig. 15(a), the harmonics are concentrated around the carrier frequency and it's multiple. The first harmonic for the proposed controller appear around 10 kHz which is the triangular frequency of the torque loop controller. This is due to the torque switching is more dominant than flux switching in DTC control scheme [32].

Figure 16 and Figure 17 show the stator phase current and stator phase current harmonic spectrum respectively for both DTC-CMLI with proposed controller and DTC-CMLI with hysteresis controller. Based on these figures, DTC-CMLI with proposed system with proposed controller produced a smoother sinusoidal stator phase current with a lower current THD compared to the DTC-CMLI with hysteresis controller.

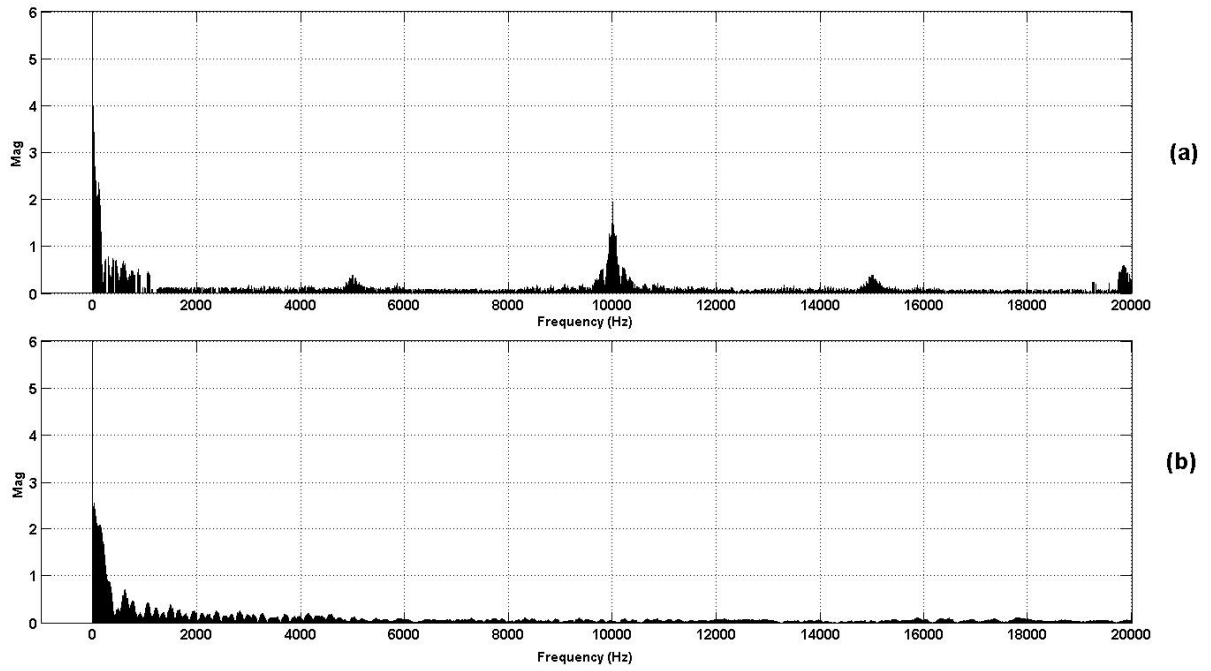


Figure 15. Frequency spectrum of the switching pattern, S_{b23} (a) Proposed controller (b) Hysteresis controller

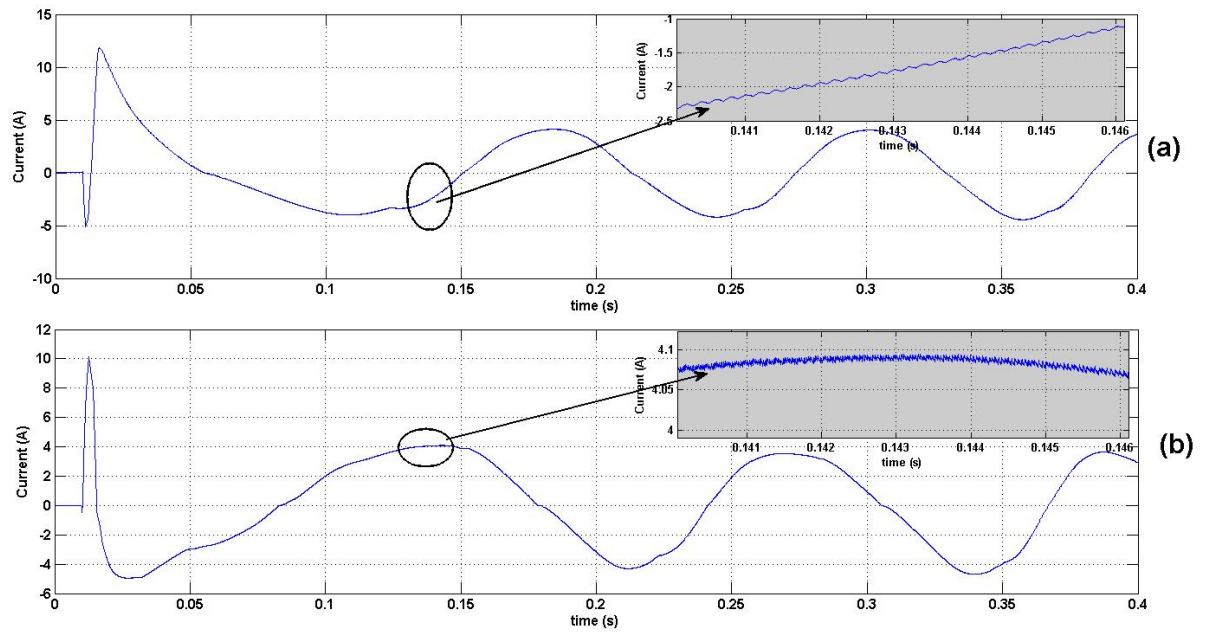


Figure 16. Stator phase current (a) Proposed controller (b) Hysteresis controller

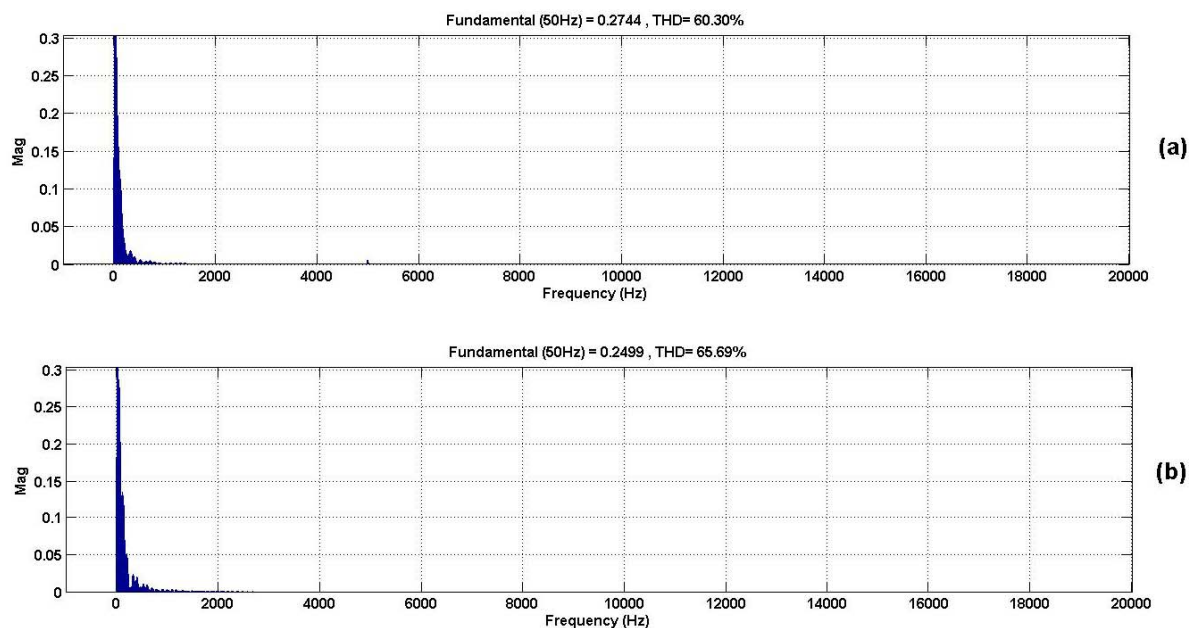


Figure 17. Stator phase current THD (a) Proposed controller (b) Hysteresis controller

6. CONCLUSION

A Fuzzy-PI with fixed switching frequency based torque and flux controller to enhance the DTC-CMLI performance has been proposed. Its operational concept has been presented. The performance of the proposed systems has been validated through simulations. From the results, with the proposed controller, the torque and flux ripples have been reduced and is capable of producing good dynamic performance. Regardless of the operating conditions, the devices' switching frequency is able to be maintained at the triangular frequency and producing low THD in stator phase current.

ACKNOWLEDGMENT

The authors would like to thank the Ministry of Higher Education of Malaysia for the financial funding of this project with vote number 78590 and the Research Management Center (RMC) of Universiti Teknologi Malaysia for their supports on research management and funding with vote number Q.J1300002525.00H87.

REFERENCES

- [1] I. Takahashi and T. Noguchi, "A new quick-response and high-efficiency control strategy of an induction motor," *IEEE Transactions on Industry Applications*, pp. 820-827, 1986.
- [2] A. Alqudah, *et al.*, "Control of variable speed drive (VSD) based on diode clamped multilevel inverter using direct torque control and fuzzy logic," in *Applied Electrical Engineering and Computing Technologies (AEECT), 2013 IEEE Jordan Conference on*, 2013, pp. 1-6.
- [3] N. F. Alias, *et al.*, "Improved performance of Direct Torque Control of Induction Machine with 3-level Neutral Point Clamped multilevel inverter," in *Electrical Machines and Systems (ICEMS), 2013 International Conference on*, 2013, pp. 2110-2114.
- [4] Y. Zhang, *et al.*, "An improved direct torque control for three-level inverter-fed induction motor sensorless drive," *Power Electronics, IEEE Transactions on*, vol. 27, pp. 1502-1513, 2012.
- [5] N. A. Azli, *et al.*, "Direct Torque Control Of Multilevel Inverter-Fed Induction Machines – A Survey," *Journal of Theoretical and Applied Information Technology*, vol. 41, pp. 060-070, 2012.

- [6] N. M. Nordin, *et al.*, "Direct Torque Control with 5-level cascaded H-bridge multilevel inverter for induction machines," in *IECON 2011 - 37th Annual Conference on IEEE Industrial Electronics Society*, Melbourne, VIC Australia, 2011, pp. 4691-4697.
- [7] A. Mortezaei, *et al.*, "Direct torque control of induction machines utilizing 3-level cascaded H-Bridge Multilevel Inverter and fuzzy logic," in *Applied Power Electronics Colloquium (LAPEC), 2011 IEEE Johor Bahru, Malaysia*, 2011, pp. 116-121.
- [8] Y. Zhang, *et al.*, "An Improved Direct Torque Control for Three-Level Inverter-Fed Induction Motor Sensorless Drive," *Power Electronics, IEEE Transactions on*, p. 1, 2010.
- [9] L. Youb, *et al.*, "A new fuzzy logic direct torque control scheme of induction motor for electrical vehicles application," in *XIX International Conference on Electrical Machines (ICEM), 2010 Rome*, 2010, pp. 1-6.
- [10] P. Urrejola, *et al.*, "Direct torque control of an 3L-NPC inverter-fed induction machine: A model predictive approach," in *IECON 2010 - 36th Annual Conference on IEEE Industrial Electronics Society* Glendale, AZ, 2010, pp. 2947-2952.
- [11] S.-X. Liu, *et al.*, "A novel fuzzy direct torque control system for three-level inverter-fed induction machine," *International Journal of Automation and Computing*, vol. 7, pp. 78-85, 2010.
- [12] F. Khoucha, *et al.*, "Hybrid cascaded H-bridge multilevel-inverter induction-motor-drive direct torque control for automotive applications," *Industrial Electronics, IEEE Transactions on*, vol. 57, pp. 892-899, 2010.
- [13] H. Alloui, *et al.*, "A three level NPC inverter with neutral point voltage balancing for induction motors Direct Torque Control," in *XIX International Conference on Electrical Machines (ICEM), 2010, Rome*, 2010, pp. 1-6.
- [14] H. F. A. Wahab and H. Sanusi, "Simulink Model of Direct Torque Control of Induction Machine," *American Journal of Applied Sciences*, vol. 5, pp. 1083-1090, 2008.
- [15] R. Zaimeddine, *et al.*, "An Improved Direct Torque Control Strategy for Induction Motor Drive," *International Journal of Electrical and Power Engineering, Medwell Journals*, vol. 1, pp. 21 - 27, 2007.
- [16] Y. Wang, *et al.*, "Direct Torque Control with Space Vector Modulation for Induction Motors Fed by Cascaded Multilevel Inverters," 2006, pp. 1575-1579.
- [17] S. Kouro, *et al.*, "Direct Torque Control With Reduced Switching Losses for Asymmetric Multilevel Inverter Fed Induction Motor Drives," 2006.
- [18] X. del Toro Garcia, *et al.*, "New DTC Control Scheme for Induction Motors fed with a Three-level Inverter," *AUTOMATIKA-ZAGREB*, vol. 46, p. 73, 2005.
- [19] M. Bendyk, *et al.*, "Investigation of direct torque control system fed by modified cascade of multilevel voltage source inverter," *IEEE Compatibility in Power Electronics*, 2005, pp. 265-272, 2005.
- [20] J. Rodríguez, *et al.*, "Direct torque control with imposed switching frequency in an 11-level cascaded inverter," *IEEE Transactions on Industrial Electronics*, vol. 51, pp. 827-833, 2004.
- [21] J. Rodr guez, *et al.*, "Simple direct torque control of induction machine using space vector modulation," *Electronics Letters*, vol. 40, 2004.
- [22] X. del Toro, *et al.*, "Direct torque control of an induction motor using a three-level inverter and fuzzy logic," in *Industrial Electronics, 2004 IEEE International Symposium on*, 2004, pp. 923-927 vol. 2.
- [23] M. A. M. Prats, *et al.*, "A switching control strategy based on output regulation subspaces for the control of induction motors using a three-level inverter," *IEEE Power Electronics Letters*, vol. 1, pp. 29-32, 2003.
- [24] C. A. Martins, *et al.*, "Switching frequency imposition and ripple reduction in DTC drives by using a multilevel converter," *IEEE Transactions on Power Electronics*, vol. 12, pp. 286 -297, 2002.
- [25] M. F. Escalante, *et al.*, "Flying capacitor multilevel inverters and DTC motor drive applications," *IEEE Transactions on Industrial Electronics*, vol. 49, pp. 809-815, 2002.
- [26] Z. Tan, *et al.*, "A direct torque control of induction motor based on three-level NPCinverter," 2001.
- [27] U. Patil, *et al.*, "Torque Ripple Minimization in Direct Torque Control Induction Motor Drive Using Space Vector Controlled Diode-clamped Multi-level Inverter," *Electric Power Components and Systems*, vol. 40, pp. 792-806, 2012.
- [28] F. Khoucha, *et al.*, "A comparison of symmetrical and asymmetrical three-phase H-bridge multilevel inverter for DTC induction motor drives," *Energy Conversion, IEEE Transactions on*, vol. 26, pp. 64-72, 2011.
- [29] G. Sheng-wei and C. Yan, "Research on torque ripple minimization strategy for direct torque control of induction motors," in *International Conference on Computer Application and System Modeling (ICCASM), 2010 Taiyuan* 2010, p. V1.

-
- [30] T. R. Obermann, *et al.*, "Deadbeat-direct torque & flux control motor drive over a wide speed, torque and flux operating space using a single control law," in *Energy Conversion Congress and Exposition (ECCE), 2010 IEEE Atlanta, GA 2010*, pp. 215-222.
- [31] S. Kouro, *et al.*, "High-performance torque and flux control for multilevel inverter fed induction motors," *IEEE Transactions on Power Electronics*, vol. 22, pp. 2116-2123, 2007.
- [32] F. Patkar, *et al.*, "A New Fuzzy-PT-based Torque Controller for DTC of Induction Motor Drives," 2006, pp. 62-66.
- [33] A. G. Perry, *et al.*, "A design method for PI-like fuzzy logic controllers for DC-DC converter," *Industrial Electronics, IEEE Transactions on*, vol. 54, pp. 2688-2696, 2007.